Simple photonics-based system for Doppler frequency shift and angle of arrival measurement

Huang, Chongjia; Chen, Hao; Chan, Erwin H.W.

Published in:
Optics Express

DOI:
10.1364/OE.389439

Published: 27/04/2020

Document Version
Publisher's PDF, also known as Version of record

Research Article | Vol. 28, No. 9 / 27 April 2020 / Optics Express 14028
Optics EXPRESS

Simple photonics-based system for Doppler frequency shift and angle of arrival measurement

CHONGJIA HUANG, HAO CHEN, AND ERWIN H. W. CHAN*

College of Engineering, IT and Environment, Charles Darwin University, Darwin NT 0909, Australia
**erwin.chan@cdu.edu.au*

Abstract: A novel photonic approach for simultaneously measuring both the Doppler frequency shift (DFS) and the angle of arrival (AOA) of a microwave signal in a radar system is presented. It has the same structure as a fiber optic link consisting of a laser, an optical modulator and a photodetector. The incoming microwave signal and a reference signal are applied to the optical modulator. Beating of the echo and reference signal sidebands at the photodetector generates a low-frequency electrical signal. The DFS and the AOA can be determined from the frequency and the power of the low-frequency electrical signal measured on an electrical spectrum analyzer. The system has a very simple structure and is low-cost. It has a wide operating frequency range and a robust performance. Experimental results demonstrate a DFS measurement at around 15 GHz with errors of less than ±0.2 Hz, and a 0° to 90° AOA measurement with less than ±1° errors.

1. Introduction

Radars are widely used in both civil and defense systems. It emits an electromagnetic wave and listens to the echo reflected by an object. The echo provides information such as the speed, the moving direction, the location and the distance of an object relative to the radar antenna, for the subsequent stage to take an appropriate action. A number of radars such as automotive radars [1] and tracking radars [2] require simultaneously measuring the object speed and location. In a tracking radar, the angle of arrival (AOA) of an echo signal needs to be determined in order to adjust the radar beam pointing direction to keep the object centered in the beam. Of course, the object velocity needs to be measured as well in order to predict the object future position. The object velocity is commonly obtained from the Doppler frequency shift (DFS), which is the frequency difference between the echo signal and the transmitted signal emitted by the radar, and is given by [2]

$$f_{DFS} = f_e - f_t = \frac{2vf_t \cos\phi}{c} \tag{1}$$

where f_e and f_t are the frequency of the echo and transmitted signal respectively, v is the absolute velocity of the object, c is the speed of light in vacuum and ϕ is the elevation angle of the radar antenna. Note that the object moving direction can also be found from the DFS. That is a positive (or negative) DFS indicates that the object is moving toward to (or away from) a radar.

Recently several photonic approaches for measuring the DFS and the AOA of a microwave signal have been reported. This is because photonics has the advantages of wide instantaneous bandwidth, low loss, lightweight and high immunity to electromagnetic interference [3,4]. It has the potential to overcome limitations in electronics approaches. Additionally, in many systems, the signal is already in the optical domain for transmission and processing, hence it is sensible to perform measurement in the optical domain. A photonics-based DFS measurement system is normally implemented using a photonic mixing approach. In this case, a portion of the transmitted signal together with an echo signal are applied to one or more optical modulators.

#389439 https://doi.org/10.1364/OE.389439
Journal © 2020 Received 30 Jan 2020; revised 10 Mar 2020; accepted 6 Apr 2020; published 24 Apr 2020

Optics EXPRESS

The DFS can be found from the frequency and phase of the system output electrical signals [5–9]. The AOA of an incoming microwave signal can be estimated based on the time or phase difference of the signal received by two antennas. Again, a photonic mixing approach can be used to down convert the incoming microwave signal into a low-frequency intermediate frequency (IF) signal so that the phase difference can be measured by an electrical phase detector [10]. Change in the phase difference of the signal received by two antennas can be converted into change in the system output amplitude, which can be measured by using an optical or electrical power meter [11–13], or a multimeter [14]. Recently reported photonics-based AOA measurement systems have a wide AOA measurement range of 165° [15] and the ability to measure the AOA of both a single tone signal and a broadband signal [16]. Since both the DFS and the AOA of an echo signal are required to determine an object velocity and its location, it is highly desirable to have a single photonic system that can accurately acquire these two pieces of information. However, until now, only two photonics-based structures have been reported for measuring DFS and AOA of a microwave signal. One structure is based on an optical phase modulator and a dual-polarization modulator connected in series, which are driven by the transmitted and echo signal, respectively [17]. It requires optical filtering for removing one sideband and fiber length matching between a polarization beam splitter and two photodetectors. Furthermore, an electrical spectrum analyzer (ESA) and an oscilloscope are required to obtain the frequency and the phase difference of the output electrical signals for DFS and AOA measurements. This increases the system complexity and cost. The other structure for DFS and AOA measurement is very complex as it involves a dual-polarization modulator and a Mach Zehnder modulator (MZM) connected in parallel, followed by two optical bandpass filters, an optical hybrid and four balanced detectors [1]. The performance of the two reported DFS and AOA measurement systems are also sensitive to change in the laser source wavelength and the optical signal polarization state.

The objective of this paper is to present and experimentally demonstrate a new photonics-based system for simultaneous DFS and AOA measurement. It is based on a fiber optic link with a reference signal and an echo signal applied to an optical modulator. The DFS and the AOA of an incoming microwave signal can be determined from the frequency and the power of the system output electrical signal measured on a low-frequency ESA. The system does not require any optical component other than a laser, an optical modulator and a photodetector in a conventional fibre optic link. It is very simple, low cost and highly mobile, which is suitable to be used in defense applications [18].

2. Topology and operation principle

The proposed DFS and AOA measurement system is depicted in Fig. 1. Continuous wave (CW) light from a laser source is launched into a dual-parallel dual-drive Mach Zehnder modulator (DP-DDMZM). The DP-DDMZM is formed by two DDMZMs in the two arms of a main MZM. An echo signal reflected by a moving object is received by two antennas, which are connected to the two input RF ports of the top DDMZM ($DDMZM_1$) inside the DP-DDMZM. The bottom DDMZM ($DDMZM_2$) is driven by a reference signal. The frequency of the reference signal should be larger than the sum of the transmitted signal frequency and twice the absolute value of the maximum possible DFS. In most applications, the DFS is within ±1 MHz [6]. Therefore, the reference signal frequency is chosen to be the transmitted signal frequency plus 2 MHz. The two DDMZMs and the main MZM are biased at the null point. Figure 2 shows the optical spectrum at the output of the two DDMZMs and the DP-DDMZM. It can be seen from the figure that the DP-DDMZM output consists of a residual optical carrier and two pairs of first order sidebands at $f_c \pm f_r$ and $f_c \pm f_e$ where f_c and f_r are the optical carrier frequency and the reference signal frequency, respectively. The amplitude of the echo signal sidebands at $f_c \pm f_e$ is dependent on the phase difference of the echo signal into the two input RF ports of $DDMZM_1$. The output of the DP-DDMZM is detected by a photodetector. This produces a photocurrent at f_r-f_e, which

Optics EXPRESS

is between 1 MHz and 3 MHz for most applications. The frequency and the power of the output frequency component at f_r-f_e can be measured by a low-frequency ESA.

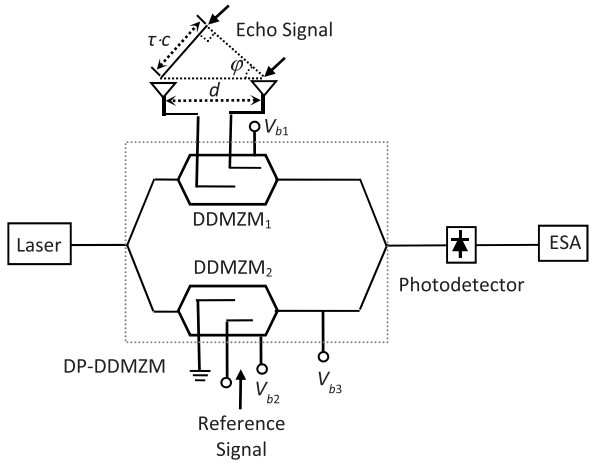

Fig. 1. Schematic diagram of the DP-DDMZM based DFS and AOA measurement system. τ is the time delay, c is the speed of light in vacuum, φ is the AOA of the echo signal, d is the antenna separation, and V_{b1}, V_{b2} and V_{b3} are the three bias voltages of the DP-DDMZM.

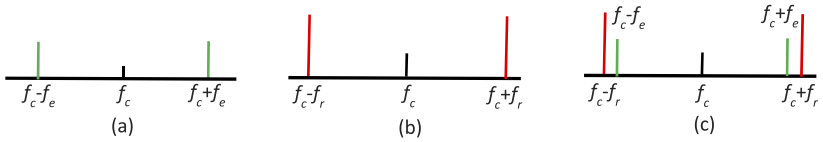

Fig. 2. Optical spectrum at the output of (a) DDMZM$_1$, (b) DDMZM$_2$ and (c) the DP-DDMZM.

Figure 3 shows a low-frequency component at f_r-f_e, which is referred to as an info peak, at the system output electrical spectrum. When an object is moving toward to the radar receiver, the frequency of the echo signal is higher than that of the transmitted signal, i.e. a positive DFS. In this case, f_r-f_e is less than 2 MHz and hence the info peak is located on the left of 2 MHz. When the object is moving away from the radar receiver, a negative DFS is obtained and f_r-f_e is larger than 2 MHz. Hence, the info peak is located on the right of 2 MHz. Since f_r=f_t+2 MHz, the DFS is 2 MHz minus the info peak frequency f_{inf}. Once the DFS has been measured, the velocity of the object can be obtained from Eq. (1) and is given by

$$v = \frac{(2MHz - f_{\inf})c}{2f_t \cos\phi} \tag{2}$$

The power of the info peak, which is dependent on the echo signal sideband amplitude, can be used to determine the AOA of the echo signal.

The proposed DFS and AOA measurement system has a very simple structure. Furthermore, unlike the system presented in [1], [17], there are no optical filtering and no length matching required in the proposed system. Moreover, only a low-frequency ESA is needed to determine both the DFS and the AOA whereas an ESA and an oscilloscope are required in the reported structures. Hence, the DP-DDMZM based DFS and AOA measurement system is low cost, and has a wide operating frequency range and a robust performance, which are required for use in a defense system [18].

Optics EXPRESS

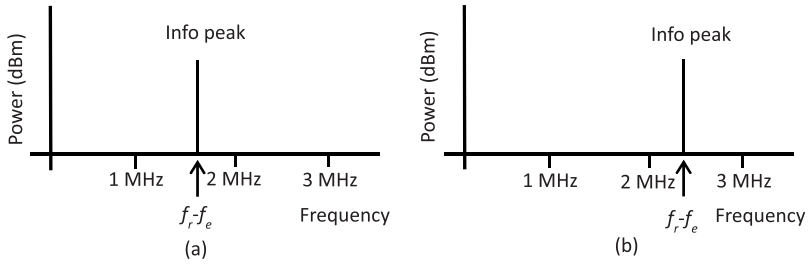

Fig. 3. System output electrical spectrum when an object is moving (a) toward to and (b) away from the radar antenna.

3. Analysis and simulation results

With reference to Fig. 1, the echo signal received by the two antennas connected to the two input RF ports of DDMZM$_1$ have a phase difference θ. The electric field at the output of DDMZM$_1$ is given by

$$E_{out1}(t) = \frac{E_{in}\sqrt{t_{ff}}}{2\sqrt{2}} e^{j2\pi f_c t} \begin{bmatrix} J_1(m_e)e^{j2\pi f_e t}(1-e^{j\theta}) - J_1(m_e)e^{-j2\pi f_e t}(1-e^{-j\theta}) \\ +J_2(m_e)e^{j4\pi f_e t}(1-e^{j2\theta}) + J_2(m_e)e^{-j4\pi f_e t}(1-e^{-j2\theta}) \end{bmatrix} \tag{3}$$

where E_{in} is the electric field amplitude of the light into the DP-DDMZM, t_{ff} is the insertion loss of the DDMZM, $J_n(m)$ is the Bessel function of nth order of the first kind, m_e=$\pi V_e/V_\pi$ is the modulation index, V_e is the voltage of the echo signal into the DDMZM and V_π is the DDMZM switching voltage. A reference signal is applied to an input RF port of DDMZM$_2$. The electric field at the output of DDMZM$_2$ is given by

$$E_{out2}(t) = \frac{E_{in}\sqrt{t_{ff}}}{2\sqrt{2}} e^{j2\pi f_c t} \begin{bmatrix} 1 - J_0(m_r) + J_1(m_r)e^{-j2\pi f_r t} - J_1(m_r)e^{j2\pi f_r t} \\ -J_2(m_r)e^{-j4\pi f_r t} - J_2(m_r)e^{j4\pi f_r t} \end{bmatrix} \tag{4}$$

where m_r=$\pi V_r/V_\pi$ is the modulation index and V_r is the voltage of the reference signal into DDMZM$_2$. The main MZM in the DP-DDMZM is biased at the null point. Hence the DP-DDMZM output electric field can be written as

$$E_{out}(t) = \frac{E_{in}\sqrt{t_{ff}}}{4} e^{j2\pi f_c t} \begin{bmatrix} -1 + J_0(m_r) + J_1(m_e)e^{j2\pi f_e t}(1-e^{j\theta}) - J_1(m_e)e^{-j2\pi f_e t}(1-e^{-j\theta}) \\ +J_2(m_e)e^{j4\pi f_e t}(1-e^{j2\theta}) + J_2(m_e)e^{-j4\pi f_e t}(1-e^{-j2\theta}) \\ +J_1(m_r)e^{j2\pi f_r t} - J_1(m_r)e^{-j2\pi f_r t} + J_2(m_r)e^{j4\pi f_r t} + J_2(m_r)e^{-j4\pi f_r t} \end{bmatrix} \tag{5}$$

The output optical signal is detected by the photodetector, which generates a photocurrent. The amplitude of the photocurrent at the frequency of f_r-f_e can be obtained from Eq. (5) and is given by

$$I_{f_r-f_e} = \Re \frac{P_{in}}{4} t_{ff} J_1(m_r) J_1(m_e) \sqrt{2[1-\cos(\theta)]} \tag{6}$$

where $\Re$ is the photodetector responsivity and P_{in} is the CW light power into the DP-DDMZM. The electrical power at the frequency of f_r-f_e, i.e. the info peak power, can be obtained from Eq. (6) and is given by

$$P_{f_r-f_e} = \frac{{P_{in}}^2}{16} {t_{ff}}^2 \Re^2 {J_1}^2(m_r) {J_1}^2(m_e) R_o [1-\cos(\theta)] \tag{7}$$

where R_o is the photodetector load resistance. Equation (7) shows the power of the info peak is dependent on the phase difference of the echo signal into the two input RF ports of DDMZM$_1$.

Optics EXPRESS

Hence the AOA of the echo signal can be obtained from the info peak power. Note that the info peak power is also dependent on the reference and echo signal modulation index, i.e. m_r and m_e. A large reference signal modulation index results in a high info peak signal-to-noise ratio (SNR). However, from Eq. (5), a large reference signal modulation index results in less optical carrier suppression. Simulation results show a reference signal modulation index of less than 0.5 is needed to ensure the optical carrier is more than 12 dB below the first order reference signal sidebands. Unlike the reference signal modulation index, the echo signal modulation index, which is determined by the voltage of the echo signal received by the antenna into $DDMZM_1$, is unknown. The echo signal voltage needs to be measured in order to determine the echo signal phase difference from the info peak power. Alternatively, a calibration process, as was described in [12,13], is needed to remove the echo signal voltage dependence in the info peak power.

The normalized power of the info peak as a function of the echo signal phase difference is plotted in Fig. 4(a). It can be seen from the figure that there is a one-to-one mapping between info peak power and the echo signal phase difference. Hence, the AOA of the echo signal can be obtained from the system output normalized info peak power. The figure also shows, for a small echo signal phase difference of less than 4°, the info peak has more than 30 dB power reduction compared to that when the echo signal phase difference is 180°. This results in more than 30 dB degradation in the SNR performance. The system parameters such as the laser source power and the reference signal modulation index need to be designed to ensure the info peak displayed on the ESA is well above the system noise floor even for a small echo signal phase difference. Note that commercial microwave signal generators have the ability to generate multiple tones in one unit. Hence both the transmitted and reference signals can be produced by a single microwave signal generator. This not only reduces the system cost but also eliminates the effect of the reference signal frequency variation on the DFS measurement because both the transmitted and reference signals share a common internal 10 MHz time base. Simulation results show there is less than 0.03 dB change in the info peak power for a 0.1 dB reference signal power variation. Hence the reference signal power stability has only little effect on the AOA measurement.

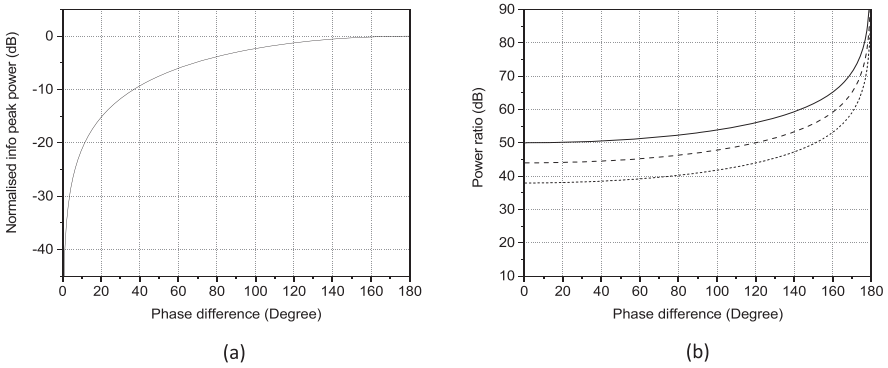

Fig. 4. (a) Normalized info peak power versus the echo signal phase difference. (b) Ratio of the info peak power and the unwanted frequency component power for 0.05 (solid), 0.1 (dashed) and 0.2 (dotted) echo signal modulation index. The reference signal modulation index is 0.5.

Note that beating of the second order echo and reference signal sidebands at the photodetector generates an unwanted frequency component at $2(f_r\text{-}f_e)$, which is close to the info peak. This could result in identifying a non-existing object. The power of this unwanted frequency component can be obtained from Eq. (5). It is given by

$$P_{2(f_r-f_e)} = \frac{{P_{in}}^2}{16} {t_{ff}}^2 \Re^2 {J_2}^2(m_r) {J_2}^2(m_e) R_o [1 - \cos(2\theta)] \tag{8}$$

Optics EXPRESS

Figure 4(b) shows the ratio of the info peak power to the unwanted frequency component power is more than 38 dB over the full 0° to 180° echo signal phase difference range when the echo signal modulation index is less than 0.2. Therefore, a frequency component at the system output spectrum can be neglected if it is located at twice the info peak frequency and has a power of more than 38 dB below the info peak.

4. Experimental results

The new DFS and AOA measurement system was set up experimentally as shown in Fig. 5. CW light with 12 dBm optical power from a 1550 nm narrow-linewidth laser (Santec WSL-100) was launched into a DP-DDMZM (Sumitomo T.SBZH1.5-20PD-ADC). An echo signal having a frequency of 15 GHz + 300 kHz from a microwave signal generator (Keysight N5173B) was equally split into two via a power splitter. Each of the two echo signals passed through an electrical phase shifter, which introduced a phase difference between the two signals to emulate an echo signal AOA, followed by an electrical variable attenuator and a 180° hybrid coupler before being applied to the two input RF ports of a DDMZM inside the DP-DDMZM. The use of the 90° and 180° hybrid couplers in the experimental setup shown in Fig. 5 enables the phase difference of the echo signals into the optical modulator to be accurately monitored on a network analyser, while measuring the info peak power at the system output. The electrical phase shifters, variable attenuators, hybrid couplers and power splitter shown in Fig. 5 are not required for the proposed system operating in practice. The other DDMZM inside the DP-DDMZM was driven by a reference signal with a frequency of 15 GHz + 2 MHz from a microwave signal generator (Analog Devices HMC-T2220). The switching voltage of the DDMZM was measured to be 3.2 V at 15 GHz. The power of the echo and reference signal into the two DDMZMs were -18 dBm and 2.6 dBm, respectively. Hence the modulation index of $DDMZM_1$ and $DDMZM_2$ were 0.04 and 0.42, respectively. The two DDMZMs and the main MZM in the DP-DDMZM were biased at the null point. The optical carrier at the output of the DP-DDMZM was more than 9 dB below the first order reference signal sidebands. The DP-DDMZM output optical signal was amplified by an erbium-doped fiber amplifier (Amonics AEDFA-PA-35-B-FA), which was followed by a 0.5 nm 3-dB bandwidth tunable optical filter (Santec OTF-320) for suppressing the amplified spontaneous emission noise. The output optical signal was detected by a photodetector (Discovery Semiconductors DSC30S) whose output was connected to an ESA (Keysight N9000A) to measure the frequency and the power of the info peak.

Figure 6 depicts the system output electrical spectrum. This shows an info peak at 1.7 MHz, which is the difference of the reference and echo signal frequency. The DFS is 2 MHz minus the info peak frequency, which is +300 kHz. A positive DFS indicates the object is moving toward to the radar. The figure also shows the power of the info peak changes from -45.9 dBm to -20.9 dBm when the electrical phase shifter was adjusted to increase the echo signal phase difference from 5° to 120°. Note the info peak in Fig. 6(a) is more than 50 dB above the system noise floor even for a small echo signal phase difference of 5°. Hence, the noise present in the system has negligible effect on the info peak power and consequently the AOA measurement accuracy. The info peak power was measured on the ESA for a 0° to 180° echo signal phase difference. Figure 7(a) shows the info peak power increases as the echo signal phase difference increases. An excellent agreement between the measured normalized info peak power and the theoretical prediction obtained from Eq. (7) can be seen. Assuming the two antennas in the actual system have a half wavelength separation, i.e. d in Fig. 1 is $\lambda/2$ where λ is the wavelength of the echo signal. Under this condition, the relationship between the echo signal AOA φ and phase difference θ is given by [10]

$$\varphi = \sin^{-1}\left(\frac{\theta}{\pi}\right) \tag{9}$$

Optics EXPRESS

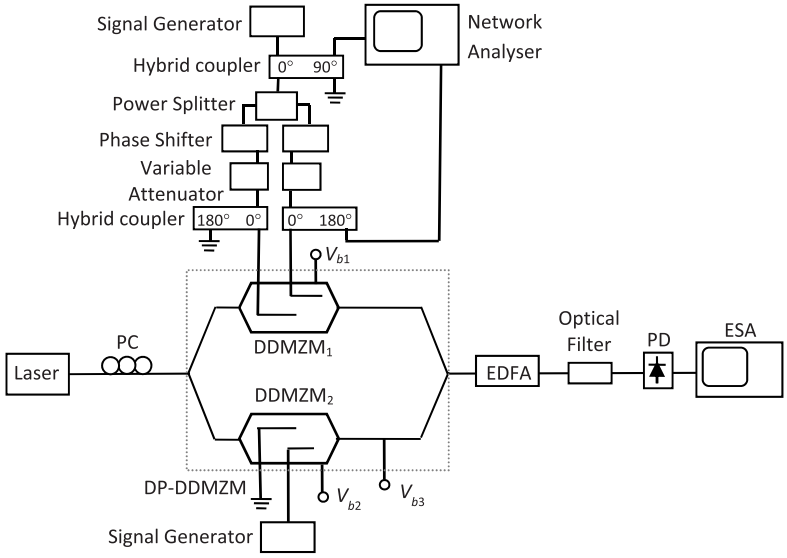

Fig. 5. Experimental setup of the proposed photonics-based system for DFS and AOA measurement.

The estimated AOA of the echo signal can be obtained based on the measured and simulated normalized info peak power, and is shown in Fig. 7(b). The result shows there are less than ±1° errors in a 0° to 90° AOA measurement range. In the ideal case, the info peak is fully eliminated at 0° echo signal phase difference. However, in practice, due to slight amplitude and phase imbalance of the signals into the two DDMZM RF input ports, the normalized info peak power is around -40 dB at 0° phase difference.

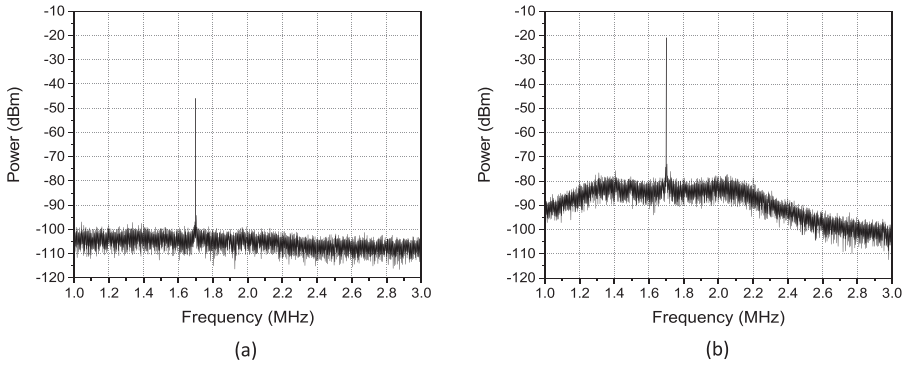

Fig. 6. Measured system output electrical spectrum for a 15 GHz + 300 kHz echo signal into the two input RF ports of the DDMZM having (a) a 5° and (b) a 120° phase difference.

The echo signal frequency was changed from 15 GHz + 300 kHz to 15 GHz - 300 kHz. Figure 8 depicts the system output electrical spectrum. In this case, the info peak is appeared at 2.3 MHz, which is larger than 2 MHz. Therefore, the DFS is -300 kHz. A negative DFS indicates the object is moving away from the radar. As shown in Fig. 8 that the power of the info peak is -46.3 dBm and -20.8 dBm for a 5° and 120° echo signal phase difference respectively, which are similar to that shown in Fig. 6 when the DFS is +300 kHz. It can be seen from Figs. 6 and 8 that the info peak is more than 50 dB above the noise floor for a 5° and 120° echo signal phase

Optics EXPRESS

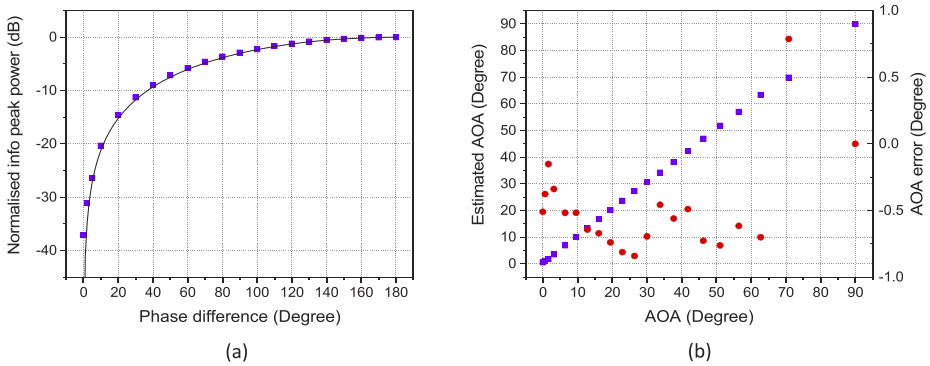

Fig. 7. (a) Measured (purple square) and simulated (sold line) normalized info peak power for a 0° to 180° echo signal phase difference. (b) Estimated AOA versus actual AOA (purple square) and corresponding error (red circle).

difference. The figures also show there is no unwanted frequency component. This is because the echo signal frequency is 15 GHz ± 300 kHz and hence the unwanted frequency component due to beating of the second order reference and echo signal sidebands at the photodetector is located at 3.4 MHz. This is outside the possible info peak frequency range of 1 to 3 MHz. Hence, the unwanted frequency component can be neglected.

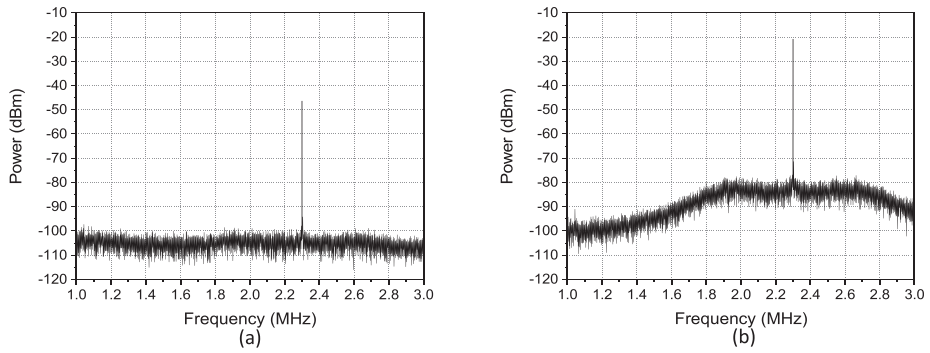

Fig. 8. Measured system output electrical spectrum for a 15 GHz - 300 kHz echo signal into the two input RF ports of the DDMZM having (a) a 5° and (b) a 120° phase difference.

Finally, the echo signal phase difference was fixed at 120° while the echo signal frequency was changed from 15 GHz - 100 kHz to 15 GHz + 100 kHz in a step of 10 kHz. The info peak frequency was measured on the ESA with a setting of 10 Hz resolution bandwidth, 10 Hz video bandwidth and 100 kHz span. Figure 9 shows the DFS measurement errors are within ±0.2 Hz. Therefore, using the proposed photonics-based system to measure the DFS and the AOA of an echo signal, the velocity of an object can be estimated with less than $\pm 4 \times 10^{-3}$ m/s errors for a 60° radar antenna elevation angle.

Optics EXPRESS

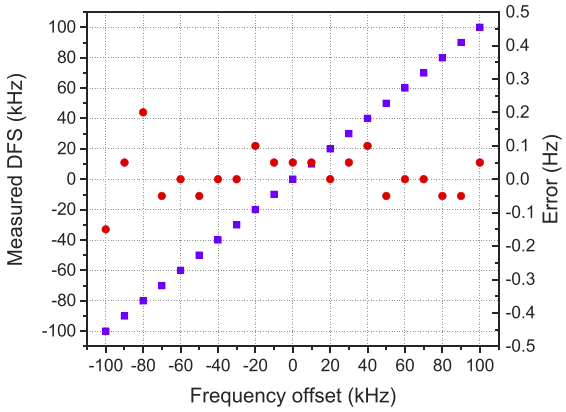

Fig. 9. Measured DFS (purple square) and corresponding error (red circle) for a 15 GHz echo signal with a frequency offset within ±100 kHz.

5. Conclusion

A new photonics-based DFS and AOA measurement system has been presented. It has a very simple structure, which is the same as a fiber optic link formed by a laser, an optical modulator and a photodetector. The system output electrical spectrum has a low-frequency info peak. The object location, speed and moving direction can be obtained based on the frequency and the power of the info peak measured on a low-frequency ESA. The system performance has been analyzed in relation to the reference signal amplitude and frequency. Experiments have been conducted to verify the proposed system. Results have been presented that demonstrate both positive and negative DFS can be measured on an ESA with less than ±0.2 Hz measurement errors for a 15 GHz echo signal with a frequency offset of ±100 kHz. Results also demonstrated an AOA measurement range from 0° to 90° with less than ±1° errors. The new photonics-based system provides a simple, low-cost, and robust DFS and AOA measurement solution, which overcomes the drawbacks of the reported structures, enabling it to be used for defense applications.

Disclosures

The authors declare no conflicts of interest.

References

1. Z. Tang and S. Pan, "Simultaneous measurement of Doppler-frequency-shift and angle-of-arrival of microwave signals for automotive radars," *2019 International Topical Meeting on Microwave Photonics (MWP)*, pp. 1–4, (2019).
2. M. I. Skolnik, "*Radar handbook*," McGraw-Hill (2008).
3. S. Pan and J. Yao, "Photonics-based broadband microwave measurement," J. Lightwave Technol. **35**(16), 3498–3513 (2017).
4. R. A. Minasian, E. H. W. Chan, and X. Yi, "Microwave photonic signal processing," Opt. Express **21**(19), 22918–22936 (2013).
5. L. Xu, Y. Yu, H. Tang, and X. Zhang, "A simplified photonic approach to measuring the microwave Doppler frequency shift," IEEE Photonics Technol. Lett. **30**(3), 246–249 (2018).
6. B. Lu, W. Pan, X. Zou, X. Yan, L. Tan, and B. Luo, "Wideband Doppler frequency shift measurement and direction ambiguity resolution using optical frequency shift and optical heterodyning," Opt. Lett. **40**(10), 2321–2324 (2015).
7. W. Chen, A. Wen, X. Li, Y. Gao, Y. Wang, S. Xiang, H. He, and H. Zheng, "Wideband Doppler frequency shift measurement and direction discrimination based on a DPMZM," IEEE Photonics J. **9**(2), 1–8 (2017).
8. C. Huang, E. H. W. Chan, and C. B. Albert, "Wideband DFS measurement using a low-frequency reference signal," IEEE Photonics Technol. Lett. **31**(20), 1643–1646 (2019).
9. B. Kang, Y. Fan, W. Wang, Z. Wang, Q. Tan, W. Jiang, Y. He, and Y. Gao, "6–40 GHz photonic microwave Doppler frequency shift measurement based on polarization multiplexing modulation and I/Q balanced detection," Opt. Commun. **456**, 124579 (2020).

Optics EXPRESS

10. P. D. Biernacki, A. Ward, L. T. Nichols, and R. D. Esman, "Microwave phase detection for angle of arrival detection using a 4-channel optical downconverter," *International Topical Meeting on Microwave Photonics (MWP)*, 137–140 (1998).
11. X. Zou, W. Li, W. Pan, B. Luo, L. Yan, and J. Yao, "Photonic approach to the measurement of time-difference-of-arrival and angle-of-arrival of a microwave signal," Opt. Lett. **37**(4), 755–757 (2012).
12. Z. Cao, H. P. A. van den Boom, R. Lu, Q. Wang, E. Tangdiongga, and A. M. J. Koonen, "Angle-of-arrival measurement of a microwave signal using parallel optical delay detector," IEEE Photonics Technol. Lett. **25**(19), 1932–1935 (2013).
13. H. Chen and E. H. W. Chan, "Angle of arrival measurement system using double RF modulation technique," IEEE Photonics J. **11**(1), 1–10 (2019).
14. H. Chen and E. H. W. Chan, "Simple approach to measure angle of arrival of a microwave signal," IEEE Photonics Technol. Lett. **31**(22), 1795–1798 (2019).
15. H. Zhou, A. Wen, and Y. Wang, "Photonic angle-of-arrival measurement without direction ambiguity based on a dual-parallel Mach–Zehnder modulator," Opt. Commun. **451**, 286–289 (2019).
16. P. Li, L. Yan, J. Ye, X. Feng, X. Zou, B. Luo, W. Pan, T. Zhou, and Z. Chen, "Angle-of-arrival estimation of microwave signals based on optical phase scanning," J. Lightwave Technol. **37**(24), 6048–6053 (2019).
17. P. Li, L. Yan, J. Ye, X. Feng, W. Pan, B. Luo, X. Zou, T. Zhou, and Z. Chen, "Photonic approach for simultaneous measurements of Doppler-frequency-shift and angle-of-arrival of microwave signals," Opt. Express **27**(6), 8709–8716 (2019).
18. J. Y. Choe, "Defense RF systems: future needs, requirements, and opportunities for photonics," *2005 International Topical Meeting on Microwave Photonics (MWP)*, pp. 307–310, (2005).